# Preliminary Results of the Portable Cold $^{87}$Rb Atomic Clock in NIM

Fasong Zheng, Kun Liu, Weiliang Chen, Shaoyang Dai and Fang Fang
Time and Frequency Division, National Institute of Metrology
Beijing 100029, China
Email: fangf@nim.ac.cn, zhengfs@nim.ac.cn

***Abstract*—A portable cold $^{87}$Rb atomic clock is under development at NIM. The clock uses $^{87}$Rb atoms which are trapped and cooled in a small three-dimensional magneto-optical trap (3D-MOT) chamber. Within the 3D-MOT chamber, the free-falling atoms are prepared in $|F=2, m_F=0\rangle$ clock state with optical pumping (OP) directly after post cooling by 2–2′ OP light and repumping. Following optical state selection, the free-falling atoms enter a microwave cavity where they undergo microwave interrogation. Eventually, the number of atoms in two clock states are detected individually by the fluorescence detection method in the detection chamber. The preliminary results show that, the selected atom number has been improved about 3 times with the optical state selection compared to the microwave state selection method. And a Ramsey fringe has been obtained experimentally, and the contrast of the central Ramsey fringe exceeds 88% with a full width half maximum (FWHM) of less than 9 Hz.**

***Keywords—time and frequency metrology, atomic clock, microwave cavity, optical pumping, Ramsey fringe***

## I. INTRODUCTION

Since the first atomic timekeeper, the microwave atomic clock became available in 1955, the microwave atomic clocks have been developed for nearly 70 years [1-3]. Microwave atomic clocks with either a hot vapor cell [4, 5] or cold-atom ensembles [6-9] were developed rapidly to generate accurate and precise time and frequency, having made considerable contributions to the fields such as communications, synchronization, financial transactions and navigation systems in modern life [10].

Compared with the hot vapor cell, laser cooled atoms with low velocities have been demonstrated to achieve a narrower linewidth under the Ramsey interrogation scheme, leading to a dramatic improvement of clock frequency performance. Among these cold atom clocks, atomic fountains have achieved the highest stability and accuracy at a few parts in $10^{16}$ [11-14]. The NIM5 Cs fountain clock developed at NIM of China has monthly reported data to BIPM since 2014, operating with a typical fractional frequency instability of $3\times10^{-13}(\tau/s)^{-1/2}$ and a Type B uncertainty of $1.4\times10^{-15}$, which is mainly dominated by the microwave-related frequency shifts [15]. However, these fountain systems are usually complex, large in size and heavy in weight.

Many applications demand the microwave atomic clocks to be robust and having the features of compact size, low weight and low power consumption. Also, they are expected with accuracy and short- and long-term stability comparable to the best current primary standards. Thus, compact cold atoms clocks have attracted extensive research attention in the past two decades, and are targeted for release into commercial market [8, 9, 16]. In our lab, we attempt to develop a portable free-falling-typed cold-atom microwave clock.

This work was supported by National Natural Science Foundation of China Youth Science Foundation Project under Grant 12303074, Key R&D Projects of the Ministry of Science and Technology under Grant 2021YFF0603800, and Fundamental Research Funds of NIM under Grant AKYJJ2402.

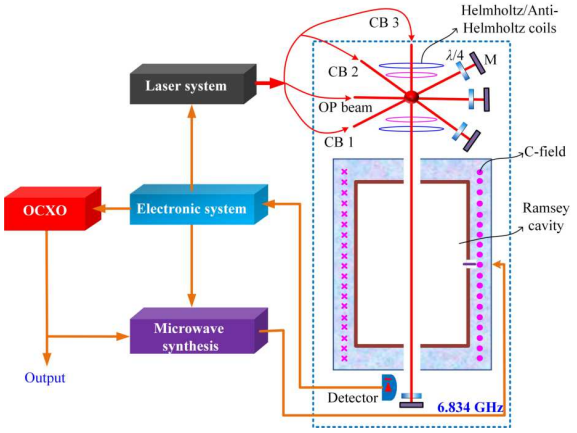


Fig. 1: Block diagram of the portable cold $^{87}$Rb atomic clock. CB, cooling beam; OCXO, oven-controlled crystal oscillator.

## II. EXPERIMENTAL SET UP AND PRINCIPLES

### A. Working Principle

A block diagram of the portable cold $^{87}$Rb atomic clock is shown in Fig.1. The $^{87}$Rb atoms are trapped and cooled in a small three-dimensional magneto-optical trap (3D-MOT) chamber. Within the 3D MOT chamber, the free-falling atoms are prepared in $|F=2, m_F=0\rangle$ clock state with optical pumping (OP) directly after post cooling by 2–2′ OP light and repumping. Following optical state selection, the free-falling atoms enter a microwave cavity where they undergo microwave interrogation. After the microwave interrogation sequence, the microwave-interrogated atoms in two clock states are detected individually by the fluorescence normalized detection method in the detection chamber. This signal is then used to control the frequency output of the clock.

### B. Optical Pumping Principle for State Selection

The $^{87}$Rb D2 line transitions used for the clock are shown in Fig. 2. A π-polarized laser with its polarization direction aligned with the direction of the magnetic field generated by the Helmholtz coil is applied to drive the $|F=2\rangle\rightarrow|F'=2\rangle$ transition. The forbidden transition of $|F=2,m_F=0\rangle\rightarrow|F'=2, m_F=0\rangle$ leads to a population accumulation in the $|F=2, m_F=0\rangle$ state (Fig. 3). A π-polarized laser resonant with $|F=1\rangle\rightarrow|F'=2\rangle$ transition is used as the repump laser to repump the atoms back to the $|F=2\rangle$ state from the $|F=1\rangle$ state. In this circumstance, the purity of linear polarization of OP laser, the coincidence between the magnetic field direction and

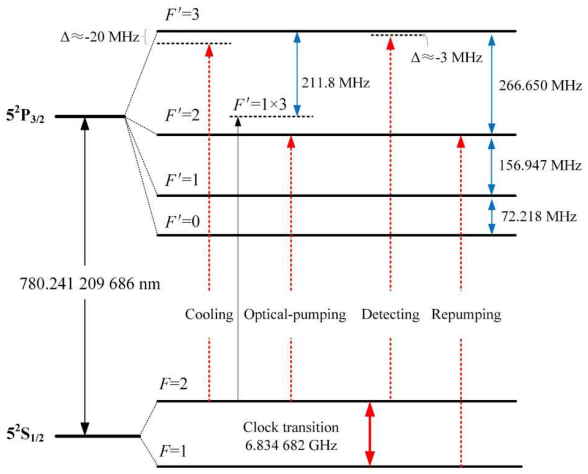


Fig. 2: $^{87}$Rb D2 line transitions used for the clock.

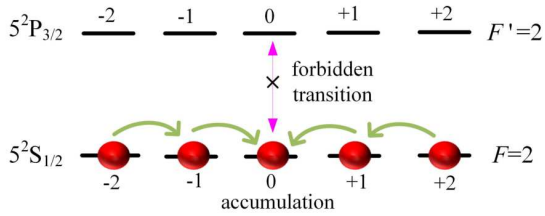


Fig. 3: Scheme of principle of optical state selection.

linear polarization direction of laser beams are the limiting factors to OP efficiency.

### C. *Normalized detection principle*

The shot-to-shot fluctuations of the number of atoms collected and detected can significantly limit the achievable signal-to-noise ratio (SNR), eventually limiting the clock frequency stability. Thus, a method of detecting normalized clock state populations in the clock is vital. Population normalization procedures have been demonstrated in the past [17-19].

In this clock, the normalized detection configuration is shown in Fig. 4. Along the free-falling path of the atomic cloud, it contains three laser beams. Two counterpropagating vertical and power-balanced beams resonant with the $|F=2\rangle \rightarrow |F'=3\rangle$ transition are the upper and lower detecting beams which are also used as the cooling beams in the cooling stage. They are used to induce fluorescence from the atoms in $|F=2\rangle$ state. The third is the repumping beam resonant with the $|F=1\rangle \rightarrow |F'=2\rangle$ transition which is used to transfer the atoms to the $|F=2\rangle$ state from $|F=1\rangle$ state. The fluorescence is collected by the two lenses and measured by the detector. The detector outputs are used to calculate the normalized transition probability.

The normalization is achieved by applying two short pulses of two counterpropagating vertical beams when the atomic cloud enters the detection region. Shown in Fig. 5, the first pulse induces fluorescence from the atoms in $|F=2\rangle$ state. A pulse of the repumping beam then swiftly transfers all the atoms to the $|F=2\rangle$ state, such that a second detection pulse induces fluorescence from the total number of atoms. A third pulse is applied at the end of the detection sequence to measure the background light. Eventually, a normalized clock transition probability $P$ can be expressed as

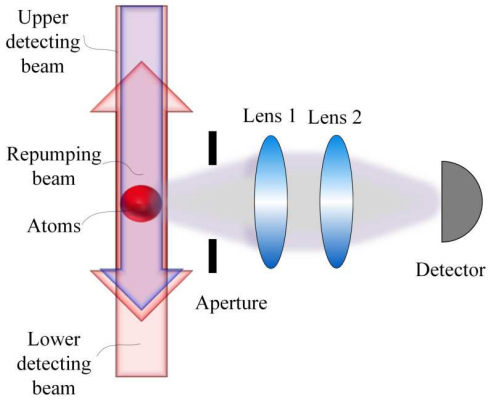


Fig. 4: Detection configuration.

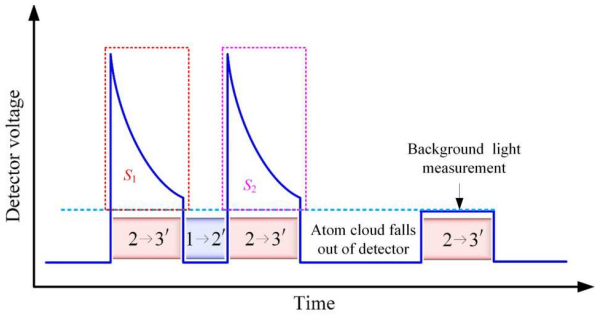


Fig. 5: Illustration of the voltage-time signal.

$$P = \frac{AS_1 + S_2}{(A+B)S_1 + S_2} \tag{1}$$

where $S_1$ and $S_2$ are the areas under the red and purple dotted boxes, respectively, after subtracting the background level (dashed line). $A$ and $B$ are constants which are related to atom temperature and detection efficiency and so on.

## III. EXPERIMENTS AND RESULTS

The curves of atom number change in $F=2$ state when sweeping the frequency of interrogation microwave with and without optical state selection, are show in Fig. 6. Without optical state selection, all the atoms in the $|F=2, m_F\rangle$ states will enter the Ramsey cavity, but only 20% of them transfer to $|F=1, m_F=0\rangle$ state under the Ramsey interrogation. And the measured transition curve is shown as the blue line in Fig. 6. With optical state selection, most atoms will be prepared in the $|F=2, m_F=0\rangle$ state then enter Ramsey cavity. Under the Ramsey interrogation, the measured transition curve is shown as the red line in Fig. 6. It shows that, the selected atom number has been improved about 3 times with the optical state selection compared to the microwave state selection method.

Also, a Ramsey fringe has been obtained experimentally under optical state selection and is shown in Fig. 7. It shows that the contrast of the central Ramsey fringe exceeds 88% with a full width half maximum (FWHM) of less than 9 Hz.

## IV. CONCLUSIONS

A portable free-falling-typed cold-atom microwave clock is developed and some preliminary result are obtained in NIM. The experimental results show that, the selected atom

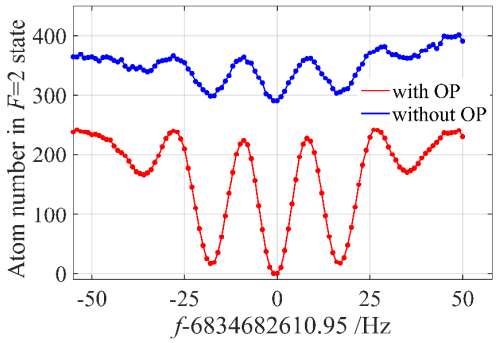


Fig. 6: Change of atom number in $F$=2 state when sweeping the frequency of interrogation microwave with and without optical state selection.

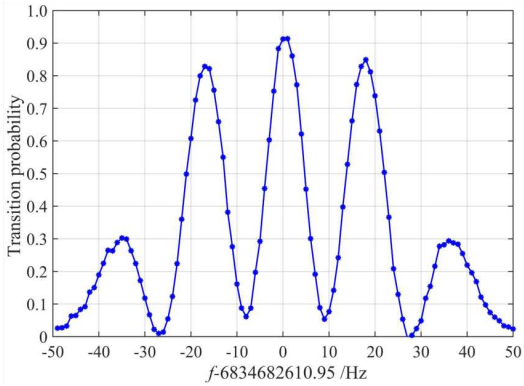


Fig. 7: Ramsey fringe of the |2, 0⟩↔|1, 0⟩ clock transition. The central fringe has a FWHM width of less than 9 Hz and a contrast of 88%.

number has been improved about 3 times with the optical state selection compared to the microwave state selection method. A Ramsey fringe has been obtained, and the contrast of the central Ramsey fringe exceeds 88% with a full width half maximum (FWHM) of less than 9 Hz. In the future, we will improve the signal-to-noise ratio (SNR) by improving the detection circuit and reducing background light, to improve frequency stability.

## ACKNOWLEDGMENT

We thank National Natural Science Foundation of China Youth Science Foundation Project under Grant 12303074, Key R&D Projects of the Ministry of Science and Technology under Grant 2021YFF0603800, and Fundamental Research Funds of NIM under Grant AKYJJ2402.

## REFERENCES

[1] L. Essen L and J. V. L. Parry, "An atomic standard of frequency and time interval: A cesium resonator," Nature, vol. 176, no. 4476, pp. 280-282, August 1955.

[2] L. S. Cutler, "Fifty years of commercial caesium clocks," Metrologia, vol. 42, no. 3, pp. S90-S99, August 2005.

[3] B. L. S. Marlow and D. R. Scherer, "A review of commercial and emerging atomic frequency standards," IEEE Trans. Ultrason. Ferroelectr. Freq. Control, vol. 68, no. 6, pp. 2007-2022, June 2021.

[4] S. Micalizio, C. E. Calosso, A. Godone and F. Levi, "Metrological characterization of the pulsed Rb clock with optical detection," Metrologia, vol. 49, no. 4, pp. 425–436, May 2012.

[5] M. A. Hafiz, G. Coget, P. Yun, S. Guerandel, E. de Clercq and R. Boudot, "A high-performance Raman-Ramsey Cs vapor cell atomic clock," J. Appl. Phys., vol. 120, no. 10, p. 104903, March 2017.

[6] R. Wynands and S. Weyers, "Atomic fountain clocks," Metrologia, vol. 42, no. 3, pp. 64–79, June 2005.

[7] F. X. Esnault, D. Holleville, N. Rossetto, S. Guerandel and N. Dimarcq, "High-stability compact atomic clock based on isotropic laser cooling," Physical Review A, vol. 82, no. 3, p. 033436, Sep. 2010.

[8] M. Y. Yu, Y. L. Meng, M. F. Ye, X. Wang, X. C. Ouyang, J. Y. Wan, L. Xiao, H. D. Cheng and L. Liu, "Development of the integrated integrating sphere cold atom clock," Chinese Physics B, vol. 28, no. 7, p. 070602, 2019.

[9] F. G. Ascarrunz, Y. O. Dudin, M. C. Delgado Aramburo, L. I. Ascarrunz, J. Savory, A. Banducci and S. R. Jefferts, "A portable cold $^{87}$Rb atomic clock with frequency instability at one day in the $10^{-15}$ range," in IEEE Int. Freq. Control Symp. (IFCS 2018), 2018, pp: 1-3.

[10] C. R. Ekstrom, J. L. Hanssen, T. B. Swanson, J. Taylor and S. Peil, "Cold-atom clocks as part of a timing ensemble," in 2014 IEEE International Frequency Control Symposium (FCS), 2014, pp. 1-4.

[11] S. Weyers, V. Gerginov, M. Kazda, J. Rahm, B. Lipphardt, G. Dobrev and K. Gibble, "Advances in the accuracy, stability, and reliability of the PTB primary fountain clocks," *Metrologia*, vol. 55, no. 6, pp. 789-805, Oct. 2018.

[12] R. J. Hendricks, F. Ozimek, K. Szymaniec, B. Nagórny, P. Dunst, J. Nawrocki, S. Beattie, B. Jian and K. Gibble, "Cs Fountain Clocks for Commercial Realizations—An Improved and Robust Design," *IEEE Trans. Ultrason. Ferroelectr. Freq. Control*, vol. 66, no. 3, pp. 624-631, March 2019.

[13] G. D. Rovera, S. Bize, B. Chupin, J. Guéna, Ph. Laurent, P. Rosenbusch, P. Uhrich and M. Abgrall, "UTC(OP) based on LNE-SYRTE atomic fountain primary frequency standards," *Metrologia*, vol. 53, no. 3, pp. S81-S88, May. 2016.

[14] T. P. Heavner, E. A. Donley, F. Levi, G. Costanzo, T. E. Parker, J. H. Shirley, N. Ashby, S. Barlow and S. R. Jefferts, "First accuracy evaluation of NIST-F2," *Metrologia*, vol. 51, no. 3, pp. 174-182, May. 2014.

[15] Fang F, Li M S, Lin P W, Chen W L, Liu N F, Lin Y G, Wang P, Liu K, Suo R and Li T C, "NIM5 Cs fountain clock and its evaluation" *Metrologia*, vol. 52, no. 4, pp. 454-468, Apr. 2015.

[16] F. X. Esnault, N. Rossetto, D. Holleville, J. Delporte and N. Dimarcq, "HORACE: A compact cold atom clock for Galileo," Advances in Space Research, vol. 47, no. 5, pp. 854-858, March 2011.

[17] S. Walby, M. Knapp, J. Whale, A. Wilson, R. Hendricks, C.J. Foot and K. Szymaniec, "Normalised Detection of Clock States by Cold Atom Recapture Method," 2022 Joint Conference of the European Frequency and Time Forum and IEEE International Frequency Control Symposium (EFTF/IFCS), Paris, France, 2022, pp. 1-3

[18] A. Clairon, P. Laurent, G. Santarelli, S. Ghezali, S. N. Lea, and M. Bahoura, "A cesium fountain frequency standard: preliminary results," IEEE Trans. on Instr. and Meas., vol. 44, no. 2, pp. 128-131, April 1995.

[19] G. W. Biedermann, X. Wu, L. Deslauriers, K. Takase and M. A.Kasevich, "Low-noise simultaneous fluorescence detection of two atomic states," Opt. Lett., vol. 34, no. 3, pp. 347-349, February 2009.